

Arene-Immobilized Ru(II)/TsDPEN Complexes: Synthesis and Applications to the Asymmetric Transfer Hydrogenation of Ketones

Simon Doherty,^{*,[a]} Julian G. Knight,^{*,[a]} Hind Alshaikh,^[b] James Wilson,^[a] Paul G. Waddell,^[a] Corinne Wills,^[a] and Casey M. Dixon^[a]

The Noyori-Ikariya (arene)Ru(II)/TsDPEN precatalyst has been anchored to amorphous silica and DAVISIL through the η^6 -coordinated arene ligand via a straightforward synthesis and the derived systems, (arene)Ru(II)/TsDPEN@silica and (arene)Ru(II)/TsDPEN@DAVISIL, form highly efficient catalysts for the asymmetric transfer hydrogenation of a range of electron-rich and electron-poor aromatic ketones, giving good conversion and excellent ee's under mild reaction conditions. Moreover, catalyst generated in situ immediately prior to addition of substrate and hydrogen donor, by reaction of silica-supported

[(arene)RuCl₂]₂ with (S,S)-TsDPEN, was as efficient as that generated from its preformed counterpart [(arene)Ru{(S,S)-TsDPEN}Cl]@silica. Gratifyingly, the initial TOFs (up to 1085 h⁻¹) and ee's (96–97%) obtained with these catalysts either rivalled or outperformed those previously reported for catalysts supported by either silica or polymer immobilized through one of the nitrogen atoms of TsDPEN. While the high ee's were also maintained during recycle studies, the conversion dropped steadily over the first three runs due to gradual leaching of the ruthenium.

Introduction

The asymmetric hydrogenation of ketones to alcohols is a pivotal transformation in organic synthesis which is widely used in the production of intermediates and pharmaceuticals.^[1] The Noyori arene-Ru(II)/TsDPEN system is among the most versatile and efficient catalysts for asymmetric transfer hydrogenation (ATH),^[2] using either an azeotropic mixture of formic acid and triethylamine or propan-2-ol as the hydrogen source, as well as asymmetric hydrogenation (AH)^[3] and as such numerous modifications have been reported.^[4] Although the Noyori-Ikariya catalyst is highly efficient and has been successfully applied in synthetic methodology,^[5] the catalyst can be quite costly due to the high catalyst loadings that are often required (0.5–1.0 mol%) coupled with the expense of the precious metal and a chiral ligand. As such there has been considerable interest in exploring strategies to immobilize this system onto a solid support to facilitate catalyst separation, recovery and reuse as well as improve product purification and enable integration into a continuous flow process for scale up, all of which will

ultimately reduce operating costs. One of the most popular approaches to immobilize these systems has been covalent attachment of a nitrogen-modified TsDPEN to an amorphous or mesoporous silica, while retaining the essential key feature of an 'active N–H'.^[6] In addition, while TsDPEN grafted by covalent attachment of nitrogen to polystyrene^[7] and PEG^[8] have both been used to immobilize these catalysts with varying levels of success, Xiao developed an alternative approach to immobilizing TsDPEN by attachment to poly(ethylene glycol) via both of its phenyl rings; the corresponding Noyori-Ikariya catalyst is among the most efficient to be reported with fast reaction rates, excellent ee's and outstanding reusability.^[9] Other methods used to immobilize (arene)Ru(II)/TsDPEN and facilitate its recovery and reuse include modification of TsDPEN with an imidazolium^[10] or phosphonium^[11] group for use in ionic liquids and water, respectively, and incorporation of the diamine into a Fréchet-type core-functionalized dendrimer.^[12] In more recent developments, (arene)Ru(II)/TsDPEN has been anchored to a support which also incorporates a palladium-based catalyst for cross-coupling and the resulting switchable bifunctional system used as a catalyst for enantioselective cascade reaction sequences.^[13]

In contrast to the myriad of examples of solid-supported Noyori-Ikariya-type catalysts immobilized through the TsDPEN ligand, there appears to be only a single report of immobilization through the π -arene ring.^[14] This system was prepared by polymerization of methacrylate side chain-modified [(arene)RuCl₂]₂ with ethyleneglycol dimethacrylate and the resulting polymers combined with TsDPEN to form an efficient catalyst for the ATH of ketones. However, to the best of our knowledge there are no reports of silica-supported precatalysts tethered via the η^6 -coordinated arene, which is somewhat surprising considering there are numerous advantages associated with the

[a] Dr. S. Doherty, Dr. J. G. Knight, J. Wilson, Dr. P. G. Waddell, Dr. C. Wills, Dr. C. M. Dixon
Newcastle University Centre for Catalysis (NUCAT)
School of Chemistry, Bedson Building, Newcastle University
Newcastle upon Tyne, NE1 7RU, UK
E-mail: simon.doherty@ncl.ac.uk
julian.knight@ncl.ac.uk
www.ncl.ac.uk/nes/staff/profile/simondoherty.html#background

[b] Dr. H. Alshaikh
Department of Chemistry, Science and Arts College, King Abdulaziz University, Rabigh Campus, Jeddah 21911, Saudi Arabia

Supporting information for this article is available on the WWW under <https://doi.org/10.1002/ejic.202000948>

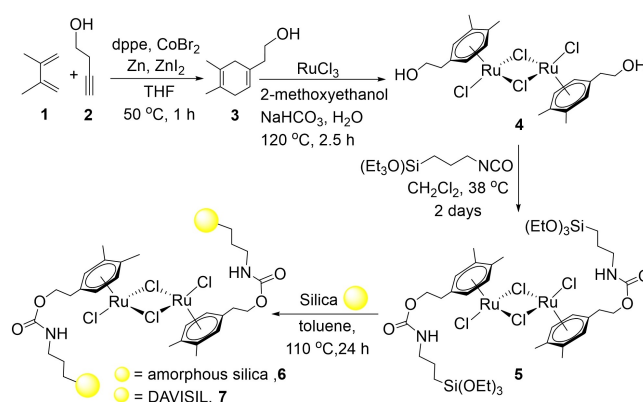
Part of the "Supported Catalysts" Special Collection.

use an ordered mesoporous silica as a support for anchoring chiral transition metal catalysts; these include control of surface area and pore volume, tunable pore dimensions, potential for functionalization and good thermal and mechanical integrity.^[15] Thus, our interest in developing such an arene-anchored catalyst is four-fold, firstly, the straightforward and versatile synthesis of a range of functionalized 1,4-cyclohexadienes via cycloaddition would lend itself to catalyst modification and diversification, secondly, a library of catalysts could be generated either before or after silanization by introduction of a suitable chiral diamine or amino alcohol, thirdly, anchoring the catalyst to the support via the arene ring avoids modification of the basic nitrogen atom of Ts-DPEN which has been reported to reduce catalyst activity and enantioselectivity and, finally, arene ruthenium complexes have also been used in a host of other transformations including; 1,4-additions to conjugated enones,^[16] hydrosilylations,^[17] arene hydrogenation,^[18] oxidation of alcohols,^[19] Diels-Alder cycloadditions,^[20] cyclopropanation,^[21] the hydrocarboxylation of alkynes^[22] and ring-opening and ring-closing metathesis^[23] and as such this strategy may well have much broader applications. Herein we report the first examples of an (arene)Ru(II)/TsDPEN-based Noyori-Ikariya precatalyst anchored to silica through the coordinated η^6 -arene and their application to the asymmetric transfer hydrogenation of ketones. The conversions and ee's obtained with these catalysts either rivalled or outperformed those obtained with their homogeneous counterparts as well as systems immobilized on either silica, a polymer or PEG through one of the nitrogen atoms of the TsDPEN.

Results and Discussion

Synthesis of Silica-Supported (Arene)Ru(II) Dimers (6 and 7), the Corresponding Precatalysts (8 and 9) and Molecular Precatalyst (10)

The key to immobilizing the (arene)Ru(II) fragment via the arene ligand is straightforward access to an appropriately substituted 1,4-cyclohexadiene which can be further modified to introduce a silanizable triethoxysilyl group after coordination to ruthenium (Scheme 1). This was achieved via the cobalt catalyzed cycloaddition between 2,3-dimethyl-1,3-butadiene **1** and 3-but-1-ynol **2** to afford the 1,4-cyclohexadiene **3** as a clear spectroscopically pure oil after purification by distillation (Scheme 1).^[24] The corresponding (arene)ruthenium(II) dimer **4** was prepared by reaction of **3** with ruthenium trichloride in 2-methoxyethanol and isolated as a pale orange solid in near quantitative yield by precipitation with diethyl ether. As each ruthenium fragment has a stereogenic plane, **4** could exist as a mixture of *rac* and *meso* diastereoisomers. Interestingly though, the ¹H NMR and ¹³C{¹H} NMR spectra appear to contain only one set of resonances with no evidence for a second diastereoisomer; this may be due to either (i) formation of a single diastereoisomer, (ii) rapid interconversion of a mixture of diastereoisomers via facile dissociation of the kinetically labile chloride bridges or (iii) formation of a mixture of diastereoisom-



Scheme 1. Synthesis of silica-supported (arene)Ru(II) dimers **6** and **7**.

ers that are indistinguishable by NMR spectroscopy. Crystallisation of **4** by slow evaporation of a concentrated ethanol solution at room temperature gave crystals suitable for a single-crystal X-ray study; a perspective view of the molecular structure is shown in Figure 1. The molecular structure shows that the crystal used to collect the data contains the (*S,R*) anti-diastereoisomer although this does not conclusively prove that **4** exists as a single diastereoisomer in solution. The Ru–C(arene) bond lengths fall between 2.149(3) and 2.200(3) Å with a mean value of *ca.* 2.18 Å, which is within the range reported for related complexes such as [(*p*-cymene)RuCl₂]₂ (range: 2.13(1)–2.18(2) Å; mean: *ca.* 2.16 Å),^[25] [(C₆H₅OCH₂CH₂OH)RuCl₂]₂ (range: 2.14(1)–2.21(1) Å; mean: *ca.* 2.17 Å),^[26] [1,4-C₆H₄(CH₂CO₂Et)₂]RuCl₂]₂ (range: 2.150(5)–2.182(5) Å; mean: *ca.* 2.17 Å)^[27] and [(C₆H₅CH₂CO₂H)RuCl₂]₂ (range: 2.15(1)–2.184(8) Å; mean: *ca.* 2.16 Å).^[28] The Ru–Cl bond lengths of 2.4152(8) Å (monodentate) and *ca.* 2.44 Å (bridging) are also unexceptional and similar to the mean value for those observed in this series of (arene)Ru-dimers (*ca.* 2.40 Å (monodentate) and *ca.* 2.45 Å (bridging)).

The silanizable triethoxysilane-containing extension was introduced by reaction of the alcohol **4** with triethoxy(3-isocyanatopropyl)silane to afford the corresponding carbamate **5** in 80% yield after washing the crude product with dry hexane

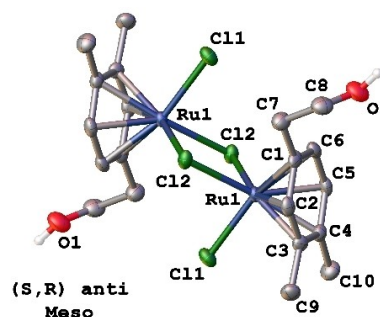


Figure 1. Crystal structure of [(2-(3,4-dimethylphenyl)ethan-1-ol)RuCl₂]₂ (**4**). Hydrogen atoms have been omitted for clarity except those of the hydroxyl groups. Ellipsoids are drawn at the 50% probability level.

to remove excess isocyanate. The identity of **5** was established by ^1H NMR spectroscopy, IR spectroscopy and the electrospray mass spectrum which contained an ion with an m/z at 534.1011 corresponding to the $[\text{Ru}(\text{arene})\text{Cl}]^+$ fragment. (Arene)Ru(II) dimer **5** is a highly versatile fragment that can be immobilised on a range of silica supports and subsequently reacted with a chiral ligand to generate a library of catalysts. Amorphous silica and DAVISIL were identified as suitable supports for our preliminary immobilisation studies; this was achieved by heating **5** and the silica in a range of solvents at reflux. Reaction times were varied and the extent of silanization determined as a function of time by filtering the reaction mixture to remove the silica and analysing the remaining solution by ^1H NMR spectroscopy, using 4-bromobenzonitrile as an internal standard to quantify the amount of **5** that had not been immobilised. The most efficient silanization was achieved in toluene after 24 h. In addition, as the π -arene ligand is known to undergo exchange at elevated temperatures, the stability of **5** in toluene was monitored at 120°C for 24 h; under these conditions there was no evidence for dissociation of the arene in **5**. Under these conditions, **5** was immobilized on amorphous silica and DAVISIL to afford **6** and **7**, respectively, in near quantitative yields. DAVISIL was chosen as it is a high surface area amorphous silica (pore size 6 nm, $450\text{--}560\text{ m}^2\text{g}^{-1}$) and as such the active sites are expected to be exposed and accessible on the surface of the support, whereas for mesoporous materials with a hierarchical structure such as MCM-41 and SBA-15 the active sites are more likely to be encapsulated in pores; moreover a wide range of pore diameters is commercially available which will ultimately enable the influence of the pore size on catalyst efficacy to be explored in a systematic manner. The amorphous silica used for comparison has a slightly smaller pore size of 4 nm and a correspondingly higher BET surface area of $>700\text{ m}^2\text{g}^{-1}$. The ruthenium loadings of **6** and **7** were determined to be 0.023 and 0.037 mmolg^{-1} , respectively, by ICP-OES which corresponds to a loading of 0.23 and $0.37\text{ wt}\%$, respectively, and the solid state ^{13}C and ^{29}Si cross-polarization magic angle spinning NMR spectra confirmed that the ruthenium dimer was immobilized onto the silica walls of an inorganosilicate network (Figure 2a).

Our interest in anchoring (arene)Ru(II) to silica through the η^6 -coordinated arene was to develop a practical system that was amenable to diversification into a library of heterogeneous catalysts by modification with a range of ligands. With the aim of demonstrating the practicality of this approach, we chose to

prepare Noyori-Ikariya-type precatalysts by reacting **6** and **7** with (*S,S*)-TsDPEN and evaluating their efficacy in the ATH of ketones. While it would be most convenient and cost effective to generate the catalyst *in situ* immediately prior to catalysis, precatalysts **8** and **9** were also first prepared on a large scale to accurately determine the ruthenium loading. Reactions were conducted in dichloromethane by stirring either **6** or **7** with a slight excess of (*S,S*)-TsDPEN and triethylamine for 4 h, in a modification of a previously reported procedure (Scheme 2).^[24a] Precatalysts **8** and **9** were isolated as pale orange solids by filtration and the ruthenium content determined to be 0.021 and 0.032 mmolg^{-1} , respectively, by ICP-OES giving loadings of 0.21 and $0.32\text{ wt}\%$. The solid state ^{13}C cross-polarization magic angle spinning NMR spectra of **8** and **9** confirmed incorporation of the (arene)Ru(II)/TsDPEN precatalyst as signals between δ 4 and 51 ppm are characteristic of the SiCH_2 , the CH_2 fragments of the aliphatic linker and the CH_3 substituents on the η^6 -arene ring and the TsDPEN, while those at δ 64 and 75 ppm correspond to the NCHPh carbon atoms of TsDPEN and the OCH_2 of the carbamate linker and those between δ 120 and 145 ppm belong to the carbon atoms of the aromatic ring of the TsDPEN and the η^6 -arene. Moreover, the chemical shifts of the structurally relevant carbon atoms map closely to those for the homogeneous molecular benchmark **10**, further confirmation for incorporation of the (arene)Ru(II)/TsDPEN precatalyst. The magic angle spinning solid state ^{29}Si spectra of **8** and **9** both contained two groups of signals typical for silica; a Q-series for inorganic silica ($\text{HO}_n\text{Si}(\text{OSi})_{4-n}$) and a T-series for organic silica $\text{RSi}(\text{OSi})_3$. The Q series appears as a set of three poorly resolved signals at *ca.* δ -91 , -102 and -112 ppm for Q_2 ($(\text{HO})_2\text{Si}(\text{OSi})_2$), Q_3 ($(\text{HO})\text{Si}(\text{OSi})_3$) and Q_4 ($\text{Si}(\text{OSi})_4$), respectively, and is markedly more intense than the major T_3 species which is a broad ill-defined peak at δ -66 ppm (Figure 2b); the disparate intensities of these resonances confirms that these catalysts are comprised mainly of inorganic silicate together with a minor amount of organic silicate resulting from immobilization of the silylated (arene)Ru(II)/TsDPEN on the walls of the silicate network. The X-ray photoelectron spectra of **8** and **9** each contained a doublet with binding energies of 462.28 eV (Ru $3p_{1/2}$) and 484.58 eV (Ru $3p_{3/2}$), and 463.78 eV (Ru $3p_{1/2}$) and 486.68 eV (Ru $3p_{3/2}$), respectively; these values are consistent with a Ru(II) species immobilized on the surface of silica.

While it is conventional to undertake comparative catalyst testing against $[(p\text{-cymene})\text{Ru}\{(\text{1S,2S})\text{-TsDPEN}\}]\text{Cl}$ as a soluble

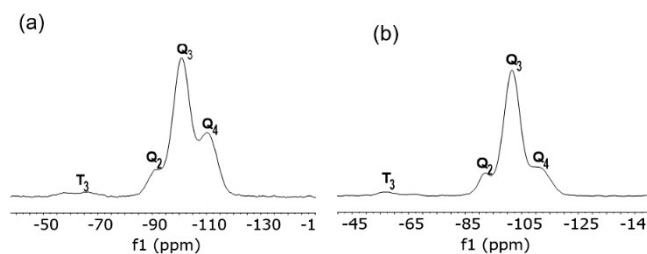
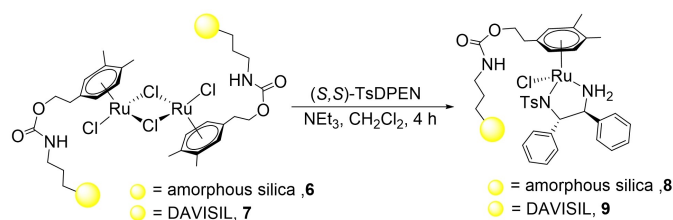


Figure 2. Solid state ^{29}Si CP MAS NMR spectra of (a) **7** and (b) precatalyst **9**.



Scheme 2. Synthesis of silica-supported (arene)Ru(II)/TsDPEN precatalysts **8** and **9**.

monomeric homogeneous pe-catalyst we chose to use [(2-(3,4-dimethylphenyl)ethan-1-ol)Ru{(1*S*,2*S*)-TsDPEN}(Cl)] (**10**) as it more closely represents a molecular analogue of **8** and **9** and, as such, should provide a more realistic assessment of the influence on catalyst performance of attachment to the support. Precatalyst **10** was prepared by stirring a dichloromethane solution of **4**, (1*S*,2*S*)-TsDPEN and triethylamine for 1 h at RT. Although the NMR spectra, the electrospray mass spectrum and analytical data were all consistent with the formulation of **10**, its identity was conclusively established by a single-crystal X-ray study; a perspective view of the molecular structure is shown in Figure 3. The molecular structure shows that the crystal used to collect the data contains a single diastereoisomer which is consistent with the NMR spectroscopic data as there is no

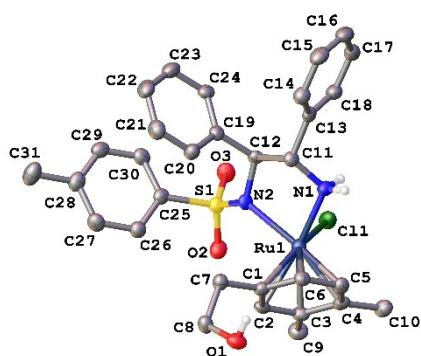


Figure 3. Crystal structure of [(2-(3,4-dimethylphenyl)ethan-1-ol)Ru{(1*S*,2*S*)-TsDPEN}(Cl)] (**10**). Hydrogen atoms have been omitted for clarity with the exception of those bound to heteroatoms. Ellipsoids are drawn at the 50% probability level.

evidence for the presence of multiple species in either the ¹H or ¹³C{¹H} NMR spectra; however, this is not conclusive as resonances may be coincident or other diastereoisomers may be present but only as a minor component. Figure 3 shows that the ruthenium atom adopts a piano stool pseudo octahedral geometry with the η⁶-arene, chloride and the (1*S*,2*S*)-DPEN completing the coordination sphere. The Ru–C(arene) bond lengths fall in the range 2.162(5)–2.217(5) Å which is consistent with those reported for related complexes such as [(*p*-cymene)Ru{(1*S*,2*S*)-TsDPEN}(Cl)] (range: 2.141(7)–2.239(8) Å; mean: *ca.* 2.19 Å),^[29] [[1,4-C₆H₄(Me)(C₄H₈OH)}Ru{(1*S*,2*S*)-TsDPEN}(Cl)] (range: 2.166(3)–2.236(3) Å; mean: *ca.* 2.20 Å),^[30] and [[C₆H₅(OCH₂CH₂OH)}Ru{(1*S*,2*S*)-TsDPEN}(Cl)] (range: 2.18(2)–2.23(2) Å; mean: *ca.* 2.2 Å).^[31] The Ru–N(1) and Ru–N(2) bond lengths of 2.104(5) Å and 2.162(4) Å, respectively, are also unexceptional and similar to those in this representative selection of precatalysts.

Asymmetric Transfer Hydrogenation of Ketones

Preliminary catalyst screening and optimization focused on acetophenone as the substrate of choice as this is often employed as the benchmark for evaluating new catalysts; optical purity and yields were determined by GC analysis and full details are listed in Table 1. Reactions were initially conducted using catalyst generated *in situ* by reaction of either **6** or **7** with a slight excess of (*S,S*)-TsDPEN and triethylamine in dichloromethane for 1 h at 55 °C, prior to addition of the reducing agent and substrate; comparative testing was also undertaken with pre-prepared catalysts **8** and **9**. Table 1 shows

Table 1. Asymmetric transfer hydrogenation of acetophenone using precatalysts generated from silica-supported ruthenium dimers **6** and **7** their precatalysts **8** and **9** or molecular precatalyst **10**.^[a]

| Entry | Catalyst system | H-donor | [Mol%] cat | Temp [°C] | Solvent | Conv. [%] (TOF [h ⁻¹]) ^[b] | ee [%] ^[b,c] |
|-------------------|---|-------------------------------------|------------|-----------|---------|---|-------------------------|
| 1 | (<i>S,S</i>)-TsDPEN/ 6 | HCO ₂ H/NEt ₃ | 0.22 | 55 | – | 90 (272) | 96 |
| 2 | (<i>S,S</i>)-TsDPEN/ 7 | HCO ₂ H/NEt ₃ | 0.34 | 55 | – | 99 (194) | 97 |
| 3 | 8 | HCO ₂ H/NEt ₃ | 0.22 | 55 | – | 88 (266) | 97 |
| 4 | 9 | HCO ₂ H/NEt ₃ | 0.34 | 55 | – | 98 (192) | 97 |
| 5 | 10 | HCO ₂ H/NEt ₃ | 1.0 | 55 | – | 99 (66) | 96 |
| 6 | (<i>R,R</i>)-Ph-pyBOX/ 7 | HCO ₂ H/NEt ₃ | 0.34 | 55 | – | 2 (3) | nd |
| 7 | (1 <i>R</i> ,2 <i>S</i>)-1-amino-2-indanol/ 7 | HCO ₂ H/NEt ₃ | 0.34 | 55 | – | 3 (6) | nd |
| 8 | (<i>S,S</i>)-TsCYDN/ 7 | HCO ₂ H/NEt ₃ | 0.34 | 55 | – | 49 (96) | 90 |
| 9 | 9 | HCO ₂ H/NEt ₃ | 0.17 | 55 | – | 77 (392) | 97 |
| 10 | 9 | Me ₂ NBH ₃ | 0.17 | 55 | – | 99 (388) | 7 |
| 11 | 9 | NaBH ₄ | 0.17 | 55 | water | 98 (384) | 3 |
| 12 | 9 | KO ₂ CH | 0.17 | 55 | water | 5 (20) | 91 |
| 13 | 9 | NH ₄ O ₂ CH | 0.17 | 55 | water | 0 (0) | nd |
| 14 | 9 | HCO ₂ H | 0.17 | 55 | – | 0 (0) | nd |
| 15 | 9 | HCO ₂ H/NEt ₃ | 0.085 | 55 | – | 26 (203) | 99 |
| 16 | 9 | HCO ₂ H/NEt ₃ | 0.17 | 50 | – | 46 (180) | 98 |
| 17 | 9 | HCO ₂ H/NEt ₃ | 0.17 | 45 | – | 18 (71) | 98 |
| 18 ^[d] | 9 | HCO ₂ H/NEt ₃ | 0.17 | 25 | – | 50 (12) | 98 |
| 19 | 9 | HCO ₂ H/NEt ₃ | 0.17 | 55 | water | 0 (0) | nd |
| 20 | 9 | HCO ₂ H/NEt ₃ | 0.17 | 55 | EtOH | 14 (55) | 49 |
| 21 | 9 | HCO ₂ H/NEt ₃ | 0.17 | 55 | MeOH | 12 (47) | 54 |

[a] Reactions were carried out with 0.5 mmol of acetophenone using precatalyst generated from silica-supported ruthenium dimers **6** and **7** or pre-prepared silica-supported (arene)Ru/TsDPEN precatalysts **8**, **9** or **10** in neat HCOOH-NEt₃ azeotrope for 90 min (unless otherwise stated) under the specified conditions of temperature, S/C ratio, hydrogen donor and solvent. [b] Determined by gas chromatography equipped with a CP-Chirasil-DEX CB column using decane as internal standard. [c] Configuration was determined to be *S* from the sign of the optical rotation. [d] Reaction time of 24 h.

that catalysts generated from either **6** or **7** and (*S,S*)-TsDPEN gave TOFs and ee's that either matched or outperformed those obtained with their soluble molecular counterpart **10**, after 1.5 h at 55 °C using formic acid-triethylamine azeotrope as the hydrogen donor (Table 1, entries 1–2 and 5). Moreover, the ee's and yields obtained with both silica-supported systems match those reported for catalyst generated from [(*p*-cymene)Ru{(*S,S*)-TsDPEN}(Cl)} and triethylamine at a reaction temperature of 60 °C,^[2b] and either compete with or outperform existing silica-supported (arene)Ru/TsDPEN-based catalysts immobilized through the nitrogen atom of the TsDPEN ligand, including magnetically retrievable mesoporous silica microcapsules^[6c,h] and (arene)Ru/TsDPEN confined in amphiphilic-modified nanocages of SBA-16,^[32a,b] or supported on silica gel, mesoporous MCM-41, SBA-15,^[6e,d,f,g] or siliceous mesocellular foam (SMF).^[6h,i] Reassuringly, the ee's and TOF's obtained with preformed catalysts **8** and **9** also match those obtained with catalyst generated *in situ* which suggests that *in situ* formation of the catalyst under these conditions is efficient and essentially quantitative (Table 1, entries 3 and 4). The slightly higher yield obtained with **9** compared to **8** is most likely due to the increased efficiency in ruthenium loading, however, at this early stage, speculation as to the origin of minor differences in activity between catalyst supported on amorphous silica and Davisil is not warranted. However, DAVISIL-supported **9** was identified as the system of choice to undertake further studies and substrate screening (*vide infra*) as the more tightly controlled chemical and structural properties of DAVISIL silicas will enable a systematic investigation of the influence of the support on catalyst efficacy to be conducted. A survey of catalysts generated *in situ* by addition of various chiral diamines and amino alcohols including (*S,S*)-TsDPEN, (*R,R*)-Ph-pyBOX, (1*R*,2*S*)-1-amino-2-indanol and (*S,S*)-TsCYDN revealed (*S,S*)-TsDPEN generated the most efficient catalyst. Following this, precatalyst **9** was used to further explore the influence of varying reaction conditions and reagents on catalyst performance including solvent, temperature, time, catalyst loading and hydrogen donor. Variation of the hydrogen donor revealed that formic acid-triethylamine azeotrope gave the best combination of TOF and ee whereas NaBH₄ and Me₂NHBH₃ both gave near quantitative yields but very poor ee's and formate salts gave negligibly low conversions. As expected, lowering the reaction temperature resulted in a reduction in activity such that a conversion of 46% was reached at 50 °C with a slight improvement in the ee to 98%; the conversion could be improved by extending the reaction time with no loss in ee. Lowering the reaction temperature further to 45 °C resulted in a marked reduction in conversion to 18% after 1.5 h which increased to 81% after 5 h, in both cases with an ee of 98%. Finally, at 25 °C a reaction time of 24 h was required to reach 50% conversion with an ee of 98%; although more sluggish than reactions conducted at higher temperatures, the enantioselectivity and TOF were comparable to those obtained by Noyori using 0.5 mol% [(*η*⁶-mesitylene)Ru{(*S,S*)-TsDPEN}(Cl)} as precatalyst.^[2b] A reduction in the catalyst loading to 0.17 mol% resulted in a slightly lower conversion of 77% with an enantioselectivity of 97% while a further reduction in the loading to 0.085 mol%

gave a much lower conversion of 26% but with an enantioselectivity of 99%. As there have been several reports of efficient ATH of ketones and imines in water using catalysts generated from silica-supported TsDPEN^[6c,d,h,32a,b] a series of reactions were conducted in water, ethanol and methanol; however, in each case conversions were either low or negligible and, as such, all further reactions were performed in neat HCOOH-NEt₃ azeotrope. A study of the conversion and ee as a function of time using 0.17 mol% **9** in neat HCOOH/NEt₃ azeotrope at 50 °C revealed that complete conversion was achieved after 2 h, which corresponds to an initial TOF of 1085 h⁻¹ (Figure 4, conversion ■ and ee ▲). For comparison, the corresponding conversion-time profile using 0.17 mol% **10** gave a markedly lower initial TOF of 260 h⁻¹ (Figure 4, conversion ● and ee ◆).

The improved performance of **9** compared with **10** could be due to either 'confinement',^[33] site isolation^[34] or preorganization of the C–H/ π interaction arising from attachment of the η^6 -arene ring to the silica^[4m,35] and further catalyst modifications are currently underway to explore the origin of this enhancement. Gratifyingly, the TOF obtained with **9** also appears to be significantly higher than Noyori-Ikariya catalysts immobilized on mesoporous silica,^[6f,h–i,7g,9a,32b] polystyrene,^[7b,d,f] or polyethylene glycol.^[8a–c,9b] Based on the above screening study, a temperature of 50 °C and reaction time of 5 h was considered to be the best compromise to explore the substrate scope and efficacy of DAVISIL silica-supported **9**.

Having identified optimum conditions and obtained encouraging conversions and ee's for the benchmark transfer hydrogenation of acetophenone, catalyst testing was extended to a range of aryl and heteroaryl ketones to explore and assess the scope and limitations of DAVISIL-supported precatalyst **9** and its molecular counterpart **10** (Table 2). Good to excellent conversions and high ee's to the corresponding secondary alcohol were obtained across a range of electron deficient 2-, 3- and 4-substituted ketones (Table 2, entries 1–10) and in most cases, silica-supported **9** either rivalled or outperformed its molecular counterpart **10**. Moreover, the TOFs and ee obtained with **9** are comparable to or better than those previously reported for (arene)Ru/TsDPEN precatalysts supported on mesoporous silica^[6c,d,e,g] and siliceous mesocellular foam^[6h,i] and encapsulated within nanocages of amphiphilic SBA-16^[32] as well as PEG-based polymers^[8a,b,c,9b] and styrene-based systems such

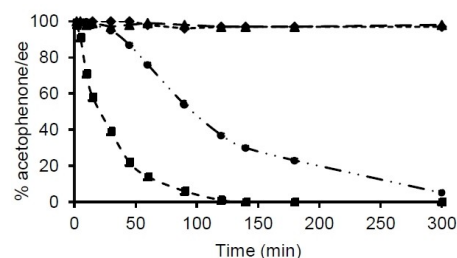
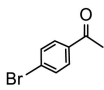
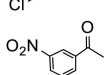
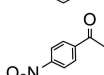
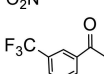
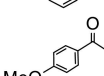


Figure 4. Reaction profile as a function of time for the asymmetric transfer hydrogenation of acetophenone in neat HCOOH/NEt₃ azeotrope using (a) 0.17 mol% **9** (%conversion ■ and %ee ▲) and (b) 0.17 mol% **10** (% conversion ● and % ee ◆).

Table 2. Asymmetric Transfer Hydrogenation of Ketones in Formic Acid-Triethylamine Azeotrope using Silica-Supported Precatalyst **9** and Molecular Precatalyst **10**.^[a]

| Entry | Substrate | Precatalyst 9 Conv [%]/(TOF [h ⁻¹]) ^[b] | ee [%] ^[b,c] | Precatalyst 10 Conv [%]/(TOF [h ⁻¹]) ^[b] | ee [%] ^[b,c] |
|-------|---|---|----------------------------|--|----------------------------|
| 1 |  | 100 (118) | 93 | 95 (112) | 92 |
| 2 |  | 99 (116) | 98 | 100 (118) | 75 |
| 3 |  | 91 (107) | 94 | 100 (118) | 94 |
| 4 |  | 100 (118) | 94 | 100 (118) | 95 |
| 5 |  | 100 (118) | 92 | 100 (118) | 90 |
| 6 |  | 80 (92) | 87 | 95 (112) | 83 |
| 7 |  | 100 (118) | 96 | 100 (118) | 93 |
| 8 |  | 100 (118) | 80 | 98 (115) | 79 |
| 9 |  | 99 (116) | 97 | 96 (113) | 97 |
| 10 |  | 99 (116) | 93 | 100 (118) | 93 |
| 11 |  | 60 (71) | > 99 | 90 (106) | > 99 |
| 12 |  | 100 (118) | > 99 | 100 (118) | > 99 |
| 13 |  | 98 (115) | 99 | 99 (116) | 99 |
| 14 |  | 100 (118) | 97 | 100 (118) | 98 |
| 15 |  | 91 (107) | 100 | 95 (112) | 99 |
| 16 |  | 78 (92) | 100 | 88 (103) | 97 |

[a] Reactions conditions: 0.5 mmol of acetophenone, 0.17 mol% silica supported (arene)Ru/Ts-DPEN precatalyst **9**, in neat 5:2 formic acid:triethylamine (0.25 mL, 3.0 mmol of HCO₂H), 50 °C, 5 h. [b] Determined by gas chromatography equipped with a CP-Chirasil-DEX CB column using decane as internal standard. [c] Configuration determined to be *S* from the sign of the optical rotation.

as a poly(styrene-1-phosphonate styrene) inorganic zirconium phosphite-phosphonate hybrid,^[7a] phosphonate-containing polystyrene copolymer,^[7b] cross-linked polystyrene,^[7d] and amphiphilic polystyrene.^[7f] While high ee's were obtained with each of the 4-substituted acetophenones examined, the ee's obtained with their 2-substituted counterparts were more

disparate and varied between 87–98%. For example, reduction of 2-bromoacetophenone gave 1-(2-bromophenyl)ethan-1-ol with an ee of 98% whereas its 2-chloro-substituted counterpart gave the corresponding secondary alcohol in 87% ee. High conversions and excellent ee's were also obtained for arylketones substituted with electron donating groups at the 2-, 3- and 4-positions (Table 2, entries 11–13) as well as 2-acetonaphthone (Table 2, entry 14) all of which gave the corresponding alcohol in 99–100% ee. Even though the *p*-methoxyacetophenone only reached 60% conversion after 5 h under these conditions (Table 2, entry 11), the ee of 99% is an improvement on that reported for [(*η*⁶-mesitylene)Ru{(S,S)-TsDPEN}Cl]^[2b] as well as the majority of silica,^[6] polymer^[7,14] and PEG-supported^[8] catalysts; moreover, complete conversion was obtained by extending the reaction time to 12 h with no loss in ee. The same protocol was extended to the asymmetric transfer hydrogenation of 2-acetylfuran and 2-acetylthiophene which gave 91% and 78% conversion to (*S*)-1-(2-furyl)ethanol and (*S*)-1-(2-thienyl)ethanol, respectively, both with 100% ee (Table 2, entries 15 and 16). While **9** tolerated the steric hindrance of a variety of *ortho*-substituted acetophenones, negligible conversions were obtained with 2,2-dimethyl-1-phenylpropan-1-one, 1-tetralone, 1-acetonaphthone, and cyclopropyl(phenyl) methanone, which are sterically much more demanding substrates. Unfortunately, **9** was also unable to reduce 3- and 4-acetylpyridine as quantitative amounts of starting material were consistently recovered even after an extended reaction time of 10 h. Reasoning that the presence of a large excess of nitrogen donor could result in ligand substitution of either the TsDPEN or chloride and afford a less active or inactive pyridine-saturated species, pre-treatment of a mixture of 0.17 mol% **9** and HCO₂H/NEt₃ azeotrope with 0.5 mmol of 3-acetylpyridine at 50 °C for 15 min resulted in a significant reduction in activity as a conversion of only 14% with an ee of 98% was obtained for the reduction of acetophenone, compared with complete conversion and an ee of 98% under the same conditions but in the absence of 3-acetylpyridine. In a modification of this investigation, the conversion of acetophenone as a function of 3-acetylpyridine addition time was investigated by running a series of hydrogenations in parallel and adding 3-acetylpyridine after 0.5 h, 1 h and 2 h and working each reaction up after 5 h; the conversion profile of 54% (0.5 h), 81% (1 h) and 98% (2 h) shows that addition of 3-acetylpyridine results in near instantaneous deactivation of the catalyst as the conversions obtained at each time interval are similar to those obtained for the same reaction in the absence of 3-acetylpyridine. In a scale-up experiment, the asymmetric transfer hydrogenation of 2-bromoacetophenone on a 10 mmol scale in 5.0 mL of the HCO₂H/NEt₃ azeotrope gave complete conversion to 1-(2-bromophenyl)ethan-1-ol with an ee of 98% after 9 h at 50 °C.

The reusability of **9** was investigated for the benchmark transfer hydrogenation of acetophenone under the conditions described above to assess the robustness and longevity of the catalyst and the potential for integration into a continuous flow reactor set-up. Recycle experiments were conducted on a larger scale to try and overcome the practical problems associated with recovering the catalyst from a small-scale reaction.

Reactions were run for 4 h to avoid complete conversion which would enable any change in activity to be observed. The catalyst was recycled by quenching the reaction with a large excess of ethyl acetate, recovering the catalyst by centrifugation, and removing the organic phase with a syringe, then recharging the flask with additional portions of HCO₂H/NEt₃ azeotrope and acetophenone.^[7d] Following this protocol, **9** gave consistently high ee's (>99%) across five cycles although conversions dropped gradually from 99% in the first run to 77% and 63% in the second and third runs, respectively, after which they remained constant (Figure 5). ICP analysis of the organic phase collected during the first three runs revealed leaching of the ruthenium to be the primary reason for the decrease in conversion as the ruthenium content dropped by 18% in run 1 and 8% and 5% in runs 2 and 3, respectively; which closely correlates with the reduction in conversion. To this end, Hintermair has recently provided convincing evidence for two deactivation/inhibition pathways for (arene)(TsDPEN)Ru–H, one of which involves gradual dissociation of the arene ligand while the other involves competitive inhibition of the unsaturated intermediate by excess base.^[36] Even though the activity dropped during the first two runs, the stable activity profile during successive runs suggests that the remaining supported ruthenium sites are robust with respect to leaching and/or deactivation and inhibition. Future studies will aim to establish why the remaining active sites are more robust after initial leaching and further improve the stability profile to integrate the system into a continuous flow process.

Conclusion

In conclusion, this paper describes the first example of a Noyori-Ikariya precatalyst anchored to amorphous silica and DAVISIL by immobilization through the η^6 -coordinated arene ligand, which was prepared via a straightforward and versatile cobalt-catalyzed [4+2] cycloaddition between a homopropargylic alcohol and a diene. The derived catalysts (arene)Ru(II)/TsDPEN@silica and (arene)Ru(II)/TsDPEN@DAVISIL exhibit excellent activity for the asymmetric transfer hydrogenation of a range of electron-rich and electron-poor aromatic ketones, giving good conversions and high ee's under mild reaction conditions. Catalyst generated *in situ*, by reaction of the corresponding silica-supported (arene)Ru(II) dimer with (S,S)-

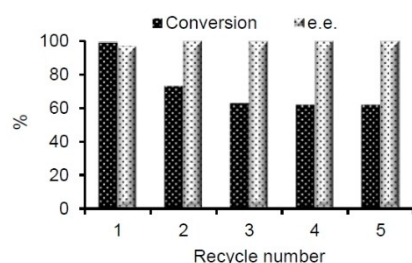


Figure 5. Recycle study for the transfer hydrogenation of acetophenone using precatalyst **9** and a reaction time of 4 h.

TsDPEN immediately prior to addition of substrate and hydrogen donor, either competed with or outperformed its preformed counterpart [(arene)Ru{(S,S)-TsDPEN}Cl]@silica, which presents numerous practical advantages for catalyst optimization, substrate screening and reaction diversification. Gratifyingly, the TOFs and ee's obtained with these catalysts rivalled those previously reported for catalysts immobilized on either silica or polymer through a nitrogen atom of the Ts-DPEN ligand. High ee's were maintained during recycle studies, however, the conversion dropped steadily over the first three runs due to gradual leaching of the ruthenium. These are encouraging results and provide a platform for further studies that will apply this immobilization strategy to prepare (arene)Ru(II)/(Ts-DPEN) precatalysts supported on a range of DAVISIL silicas as well as functionalized ordered mesoporous silicas that can be integrated into a continuous flow process for scale-up or that can be used to develop multifunctional catalysts for cascade reaction sequences and the conversion of biomass derived substrates into value-added products.

Experimental Section

Synthesis of 2-(4,5-Dimethylcyclohexa-1,4-dien-1-yl)ethan-1-ol (3). According to the literature method,^[24b] Zn powder (0.28 g, 4.22 mmol), ZnI₂ (1.40 g, 4.38 mmol), CoBr₂ (0.48 g, 2.19 mmol), and DPPE (0.86 g, 2.15 mmol) were added to a three-neck flask (250 mL) and stirred in dry THF (30 mL) at room temperature. 1,3-Dimethylbutadiene (13.5 mL, 118 mmol) was added to the reaction mixture after 5 minutes, followed by but-3-yn-1-ol (7.9 mL, 105 mmol). The resulting mixture was stirred for 5 mins and then heated to 50 °C for one hour, after which the solvent was removed under reduced pressure. The crude mixture was purified by vacuum distillation (1 mmHg, 115–121 °C) to afford diene **3** in 63% yield (10.1 g). ¹H NMR (300 MHz, CDCl₃, δ): 5.49–5.41 (m, 1H, =CH), 3.70–3.53 (m, 2H, CH₂OH), 2.63–2.39 (m, 4H, CH₂), 2.21–2.14 (m, 2H, CH₂CH₂OH), 1.60 (s, 6H, CH₃). ¹³C{¹H} NMR (75 MHz, DMSO, δ): 104.1, 102.6, 95.8, 87.5, 87.2, 83.4, 60.4, 36.2, 16.9, 16.3.

Synthesis of [RuCl₂{2-(3,4-dimethylphenyl)ethan-1-ol}]₂ (4). According to the literature,^[37] a suspension of RuCl₃·H₂O (1.1 g, 5.3 mmol) and NaHCO₃ (0.45 g, 5.3 mmol) in a mixture of 2-methoxyethanol:H₂O (11 mL, 10:1) was added 2-(4,5-dimethylcyclohexa-1,4-dien-1-yl)ethan-1-ol **3** (3.2 g, 21.2 mmol). The resulting mixture was heated at 120 °C for 2.5 h after which time half of the solvent was removed under reduced pressure and diethyl ether added (10 mL) to precipitate an orange solid. The solid was filtered, washed with Et₂O and dried to obtain the dimer **4** as an orange powder in 49% yield (0.9 g). ¹H NMR (300 MHz, DMSO, δ): 5.81 (d, *J* = 5.6 Hz, 1H, ArH), 5.70 (s, 1H, ArH), 5.58 (d, *J* = 5.6 Hz, 1H, ArH), 4.76 (t, *J* = 5.1 Hz, 1H, OH), 3.68 (qd, *J* = 6.5, 3.3 Hz, 2H, CH₂OH) 2.65–2.53 (m, 1H, CH₂CH₂CH₂OH), 2.47–2.34 (m, 1H, CH₂CH₂CH₂OH), 2.05 (s, 3H, CH₃), 1.96 (s, 3H, CH₃). ¹³C{¹H} NMR (75 MHz, DMSO, δ): 104.1, 102.7, 95.7, 87.5, 87.2, 83.3, 60.4, 36.2, 17.0, 16.3. IR: ν_{\max} cm⁻¹ 735, 863, 899, 1023, 1044, 1081, 117, 1211, 1297, 1377, 1438, 2858, 2914, 3039, 3429 (br). HRMS (ESI) calculated for C₁₂H₁₇O₃Ru [Ru(arene)OAc]⁺: 311.0220, Found: 311.0217.

Synthesis of [RuCl₂ O-(3,4-dimethylphenethyl N-(3-(triethoxysilyl)propyl) carbamate}]₂ (5). In a modification of a previously reported literature procedure,^[24a] 3-(triethoxysilyl)propyl isocyanate (0.26 mL, 1.1 mmol) was added to [RuCl₂(2-(3,4-dimethylphenyl)ethan-1-ol)]₂ (0.456 g, 0.70 mmol) and NEt₃ (0.49 mL, 3.54 mmol) in dry dichloromethane (10 mL). The reaction mixture was heated to 38 °C for

48 h. The solvent was removed under reduced pressure to obtain a brown oil which was triturated with hexane (2×10 mL). The resulting crude oil (0.645 g, 77%) was re-dissolved in dry dichloromethane (10 mL) to give a dark red solution which was used without further purification. ¹H NMR (300 MHz, CDCl₃, δ): 5.28–4.82 (m, 3H, Ar–H), 4.38–4.11 (m, 2H, CH₂CH₂O), 3.84–3.64 (m, 6H, (CH₃CH₂O)₃Si), 3.15–2.97 (m, 2H, CH₂NH), 2.90–2.69 (m, 2H, C₆H₃–CH₂CH₂O), 2.19–2.06 (m, 3H, CH₃), 2.07–1.99 (m, 3H, CH₃), 1.62–1.43 (m, 2H, NHCH₂CH₂CH₂), 1.21–1.07 (m, 9H, (CH₃CH₂O)₃Si), 0.60–0.43 (m, 6H, CH₂Si). IR: ν_{max} cm⁻¹ 3264, 2973, 2927, 2882, 1682, 1254, 1069, 951, 768. HRMS (ESI) calculated for C₂₀H₃₅O₅NCIRuSi, [Ru(arene)Cl]⁺: 534.1011, found: 534.1011.

Synthesis of Silica-Supported Ruthenium Dimers 6 and 7. A two-necked flame-dried round bottom flask was charged with 5 (4.88% w/w solution in dichloromethane; 6 mL, containing 0.34 mmol of Ru), the solvent was removed under reduced pressure and toluene (6 mL) added. Amorphous silica or DAVISIL (7.10 g) was then added to the solution and the mixture was heated to 110 °C with rapid stirring for 24 h. After this time the mixture was left to cool and the solid was filtered, washed with ethyl acetate (3×10 mL) and dried at 45 °C overnight to afford 6 and 7 as orange solids in 93% (7.45 g) and 99% (7.49 g) yield, respectively. ICP-OES data for 6: 0.23 wt% ruthenium corresponding to a ruthenium loading of 0.023 mmol g⁻¹. ICP-OES data for 7: 0.37 wt% ruthenium corresponding to a ruthenium loading of 0.037 mmol g⁻¹.

Synthesis of Silica-Supported [(2-(3,4-Dimethylphenylethyl propyl carbamate))Ru(S,S)-T-DPEN]Cl Precatalysts 8 and 9. In a typical procedure, triethylamine (0.094 mL, 0.68 mmol), silica-supported ruthenium dimer 6 or 7 (mass corresponding to 0.34 mmol of Ru calculated from the ruthenium loading) and (S,S)-TsDPEN (0.155 g, 0.42 mmol) were stirred in dichloromethane (20 mL) for 4 h at room temperature after which time the solid was filtered, washed with dichloromethane (3×5 mL) and dried in an oven at 40 °C for 5 h to obtain silica-supported precatalysts 8 and 9 as orange solids in 99% (3.7 g) and 98% (3.7 g) yield, respectively. ICP-OES data for 8: 0.21 wt% ruthenium corresponding to a ruthenium loading of 0.021 mmol g⁻¹. ICP-OES data for 9: 0.32 wt% ruthenium corresponding to a ruthenium loading of 0.032 mmol g⁻¹.

Synthesis of RuCl(S,S)-TsDPEN[(2-(3,4-dimethylphenyl)ethan-1-ol)] (10). In a modification of a previously reported literature procedure,^[24a] (S,S)-TsDPEN (0.100 g, 0.28 mmol), 4 (0.089 g, 0.14 mmol) and triethylamine (0.056 g, 0.55 mmol) were dissolved in dichloromethane (3 mL) and the reaction mixture was stirred at room temperature for 1 h. The resulting orange solid was filtered, washed with dichloromethane (1 mL) and dried to obtain precatalyst 10 as an orange solid (0.103 g, 56%). ¹H NMR (300 MHz, DMSO, δ): 7.24–7.32 (m, 1H, NH), 7.14–7.06 (m, 5H, ArH + NH), 6.83–6.54 (m, 10H, ArH), 5.74 (s, 1H, ArH), 5.62–5.59 (m, 1H, ArH), 5.44–5.43 (m, 1H, ArH), 4.91–4.89 (m, 1H, OH), 3.80–3.75 (m, 2H, CH₂OH), 3.62–3.60 (m, 1H, CHNTs), 3.16–3.10 (m, 1H, CHN), 2.92–2.86 (m, 1H, CH₃H_bCH₂OH), 2.69–2.64 (m, 1H, CH₃H_bCH₂OH), 2.22 (s, 3H, Me), 2.20 (s, 3H, Me), 2.08 (m, 3H, Me). ¹³C{¹H} NMR (75 MHz, DMSO, δ): 143.7, 140.5, 140.2, 138.6, 129.3, 128.5, 127.9, 127.9, 127.5, 127.5, 127.1, 126.4, 94.6, 94.4, 94.3, 88.7, 81.2, 79.4, 71.9, 69.3, 61.3, 36.7, 21.2, 17.1, 16.9. IR: ν_{max} cm⁻¹ 535, 575, 695, 699, 813, 918, 1064, 1129, 1265, 1422, 1453, 1575, 2875, 2925, 3028, 3056, 3243, 3301, 3433 (br). HRMS (ESI) calculated for C₃₁H₃₅N₂O₃RuS [M–Cl]⁺: 611.1439; found: 611.1440. M.P.: 221–223 °C.

ATH of Acetophenone and its Derivatives Using Preformed Silica-Supported Precatalysts 8 and 9. Ketone (0.5 mmol) was added to a suspension of either 8 (0.22 mol% Ru, 0.052 g, 0.0011 mmol) or 9 (0.34 mol% Ru, 0.053 g, 0.0017 mmol) and 5:2 formic acid:triethylamine azeotrope (0.25 mL, 3.0 mmol of HCO₂H) in a flame-dried Schlenk tube and the mixture stirred at the specified temperature

for the allocated time. The orange mixture was filtered through a short silica plug, washed through with diethyl ether (2×10 mL) and the solvent removed under reduced pressure. The residue was dissolved in CDCl₃ (0.7 mL), decane (97 μL, 0.5 mmol) added as internal standard, and the solution analysed by ¹H NMR spectroscopy and gas chromatography to determine the conversion and enantioselectivity.

ATH of Acetophenone Using In-Situ Generated Silica-Supported Precatalysts. A flame-dried Schlenk flask was charged with silica-supported ruthenium dimer 6 (0.22 mol%, 0.048 g, 0.0011 mmol) or 7 (0.34 mol%, 0.046 g, 0.0017 mmol), ligand (1.3 equivalents based on ruthenium) and triethylamine (2.0 equivalents based on ruthenium) and the resulting suspension stirred for 1 h under nitrogen at 55 °C. After this time, HCO₂H/NET₃ (0.25 mL, 3.0 mmol of HCO₂H) and the ketone (0.5 mmol) were added and the mixture stirred at 55 °C for the allocated time, after which it was filtered through silica and washed through with diethyl ether (2×10 mL) and the solvent removed under reduced pressure. The residue was dissolved in CDCl₃ (0.7 mL), decane (97 μL, 0.5 mmol) was added as internal standard and the solution analysed by ¹H NMR spectroscopy and gas chromatography to determine the conversion and enantioselectivity.

ATH of Acetophenone and its Derivatives Using Precatalyst 10. A flame-dried Schlenk flask containing 5:2 formic acid:triethylamine (0.25 mL, 3.0 mmol of HCO₂H) and the ketone (0.5 mmol) was charged with precatalyst 10 (0.0036 g, 5.5 μmol, 1 mol%) and the resulting mixture stirred at 50 °C for 5 h. After this time, the resulting orange mixture was filtered through silica and flushed with diethyl ether (2×10 mL) and the solvent removed under reduced pressure. The residue was dissolved in CDCl₃ (0.7 mL) and decane (97 μL, 0.5 mmol) added as internal standard and the solution analysed by ¹H NMR spectroscopy and gas chromatography to determine the conversion and enantioselectivity.

ATH of Acetophenone Using Precatalyst 10 Generated In-Situ from 4. A Schlenk flask was charged with 5:2 formic acid:triethylamine (0.25 mL, 3.0 mmol of HCO₂H), 4 (0.0035 g, 5.0 μmol) and (S,S)-TsDPEN (2.8 mg, 7.6 μmol) and the mixture stirred at 55 °C for 15 min. After this time, acetophenone (0.058 mL, 0.50 mmol) was added and stirring continued for a further 90 min. The resulting orange mixture was filtered through silica and flushed through with diethyl ether (2×10 mL) and the solvent removed under reduced pressure. The residue was dissolved in CDCl₃ (0.7 mL), decane (97 μL, 0.5 mmol) was added as internal and the solution analysed by ¹H NMR spectroscopy and gas chromatography to determine the conversion and enantioselectivity.

General Procedure for Catalyst Recycling. A centrifuge tube was charged with precatalyst 9 (0.17 mol%, 0.106 g, 0.0034 mmol), 5:2 formic acid:triethylamine (1.0 mL, 12.0 mmol of HCO₂H) and acetophenone (0.232 mL, 0.2 mmol) and the reaction mixture heated at 55 °C for 5 h under a nitrogen atmosphere. After this time water was added (1.0 mL) and the tube was placed in a centrifuge at 5000 rpm for 5 min and the formic acid:triethylamine carefully removed by pipette. Following this the solid was re-suspended in formic acid:triethylamine azeotrope and water, centrifugation repeated and the formic acid:triethylamine removed. After a third washing the solid was dried in vacuum before adding further portions of formic acid:triethylamine azeotrope and acetophenone. The combined aqueous washings were extracted with diethyl ether to obtain a sample for analysis by ¹H NMR spectroscopy and gas chromatography.

X-ray Crystallography

Crystal structure data were collected at 150 K on a Rigaku Oxford Diffraction Xcalibur, Altas, Gemini Ultra diffractometer using equipped with a sealed tube X-ray source ($\lambda_{\text{CuK}\alpha} = 1.54184 \text{ \AA}$) and an Oxford CryostreamPlus open-flow N_2 cooling device. Intensities were corrected for absorption using a multifaceted crystal model created by indexing the faces of the crystal for which data were collected.^[38] Cell refinement, data collection and data reduction were undertaken via the software CrysAlisPro.^[39] All structures were solved using XT^[40] and refined by XL^[41] using the Olex2 interface.^[42] All non-hydrogen atoms were refined as anisotropic and hydrogen atoms were positioned with idealised geometry, with the exception of those bound to heteroatoms, the positions of which were located using peaks in the Fourier difference map. The displacement parameters of the hydrogen atoms were constrained using a riding model with UH set to be an appropriate multiple of the Ueq value of the parent atom.

Deposition Numbers 2045014 (for **4**) and 2045015 (for **10**) contain the supplementary crystallographic data for this paper. These data are provided free of charge by the joint Cambridge Crystallographic Data Centre and Fachinformationszentrum Karlsruhe Access Structures service www.ccdc.cam.ac.uk/structures.

Acknowledgements

We gratefully acknowledge the Deanship of Scientific Research (DSR) at King Abdulaziz University, Jeddah, Saudi Arabia for funding this project (grant no: KEP-37-130-41). High-resolution mass spectra were obtained at the EPSRC National Mass Spectrometry Service in Swansea. We also thank Dr Kathryn White for the SEM images (Faculty of Medical Sciences, Newcastle University).

Conflict of Interest

The authors declare no conflict of interest.

Keywords: arene-immobilised · silica · (arene)Ru(II)/TsDPEN · asymmetric hydrogenation · ketones

- [1] a) M. J. Palmer, M. Wills, *Tetrahedron: Asymmetry* **1999**, *10*, 2045–2061; b) X. Wu, J. Xiao, *Chem. Commun.* **2007**, *24*, 2449–2466; c) H.-U. Blaser, C. Malan, B. Pugin, F. Spindler, H. Steiner, *Adv. Synth. Catal.* **2003**, *345*, 103–151; d) K. Everaere, A. Mortreux, J.-F. Carpentier, *Adv. Synth. Catal.* **2003**, *345*, 67–77; e) C. Saluzzo, M. Lemaire, *Adv. Synth. Catal.* **2002**, *344*, 915–928; f) Q.-H. Fan, Y.-M. Li, A. S. C. Chan, *Chem. Rev.* **2002**, *102*, 3385–3466.
- [2] a) S. Hashiguchi, A. Fujii, J. Takehara, T. Ikariya, R. Noyori, *J. Am. Chem. Soc.* **1995**, *117*, 7562–7563; b) A. Fujii, S. Hashiguchi, N. Uematsu, T. Ikariya, R. Noyori, *J. Am. Chem. Soc.* **1996**, *118*, 2521–2522; c) K. Matsumura, S. Hashiguchi, T. Ikariya, R. Noyori, *J. Am. Chem. Soc.* **1997**, *119*, 8738–8739; d) K. Murata, K. Okano, M. Miyagi, H. Iwane, R. Noyori, T. Ikariya, *Org. Lett.* **1999**, *1*, 1119–1121.
- [3] a) Y.-M. He, Q.-H. Fan, *Org. Biomol. Chem.* **2010**, *8*, 2497–2504; b) T. Touge, T. Arai, *J. Am. Chem. Soc.* **2016**, *138*, 11299–13105; c) T. Ohkuma, N. Utsumi, K. Tsutsumi, K. Murata, C. Sandoval, R. Noyori, *J. Am. Chem. Soc.* **2006**, *128*, 8724–8725; d) W. Ma, J. Zhang, C. Xu, F. Chen, Y.-M. He, Q.-H. Fa, *Angew. Chem. Int. Ed.* **2016**, *55*, 12891–12894; *Angew. Chem.* **2016**, *128*, 13083–13086; e) C. A. Sandoval, T. Ohkuma, N. Utsumi, K. Tsutsumi, K. Murara, R. Noyori, *Chem. Asian J.* **2006**, *1*, 102–110; f) Z. Yang, F. Chen, Y. He, N. Yang, Q.-H. Fa, *Angew. Chem. Int. Ed.* **2016**, *55*, 13863–13866; *Angew. Chem.* **2016**, *128*, 14067–14070; g) T. Ohkuma, K. Tsutsumi, N. Utsumi, N. Arai, R. Noyori, K. Murata, *Org. Lett.* **2007**, *9*, 255–257; h) M. Ito, Y. Endo, T. Ikariya, *Organometallics* **2008**, *27*, 6053–6055; i) Z. M. Heiden, T. B. Rauchfuss, *J. Am. Chem. Soc.* **2009**, *131*, 3593–3600.
- [4] For a highly informative and insightful review see: a) H. G. Nedden, A. Zanolli-Gerosa, M. Wills, *Chem. Rec.* **2016**, *16*, 2623–2643; For selected examples see: b) D. J. Cross, J. A. Kenny, I. Houson, L. Campbell, T. Walsgrove, M. Wills, *Tetrahedron: Asymmetry* **2001**, *12*, 1801–1806; c) F. K. Cheung, C. Lin, F. Minissi, A. L. Crivillé, M. A. Graham, D. J. Fox, M. Wills, *Org. Lett.* **2007**, *9*, 4659–4662; d) J. Wettergren, E. Buitrago, P. Ryberg, H. Adolffson, *Chem. Eur. J.* **2009**, *15*, 5709–5718; e) A. E. Cotman, D. Cahard, B. Mohar, *Angew. Chem. Int. Ed.* **2016**, *55*, 5294–5298; *Angew. Chem.* **2016**, *128*, 5380–5384; f) A. Kišić, M. Stephan, B. Mohar, *Adv. Synth. Catal.* **2015**, *357*, 2540–2546; g) T. Thorpe, A. J. Blacker, S. M. Brown, C. Bubert, J. Crosby, S. Fitzjohn, J. P. Muxworthy, J. M. J. Williams, *Tetrahedron Lett.* **2001**, *42*, 4041–4043; h) A. Schlatter, W.-D. Woggon, *Adv. Synth. Catal.*, **2008**, *350*, 995–1000; i) W. Baratta, F. Benedetti, A. Del Zotto, L. Fanfoni, F. Felluga, S. Magnolia, E. Putignano, P. Rigo, *Organometallics* **2010**, *29*, 3563–3570; j) X. Wu, J. Xiao, *Chem. Commun.* **2007**, 2449–2466; k) D. Šterk, M. S. Stephan, B. Mohar, *Tetrahedron: Asymmetry* **2002**, *13*, 2605–2608; l) R. Soni, K. E. Jolley, G. J. Clarkson, M. Wills, *Org. Lett.* **2013**, *15*, 5110–5113; m) V. Parekh, J. A. Ramsden, M. Wills, *Catal. Sci. Technol.* **2012**, *2*, 406–414.
- [5] a) P. A. Bradley, R. L. Carroll, Y. C. Lecouturier, R. Moore, P. Noeureuil, B. Patel, J. Snow, S. Wheeler, *Org. Process Res. Dev.* **2010**, *14*, 1326–1336; b) R. Fu, J. Chen, L.-C. Guo, J.-L. Ye, Y.-P. Ruan, P.-Q. Huang, *Org. Lett.* **2009**, *11*, 5242–5245; c) G. Kumaraswamy, G. Ramakrishna, P. Naresh, B. Jagadeesh, B. Sridhar, *J. Org. Chem.* **2009**, *74*, 8468–8471; d) T. J. Greshock, D. M. Johns, Y. Noguchi, R. M. Williams, *Org. Lett.* **2008**, *10*, 613–616; e) Q. Zhang, B.-W. Ma, Q.-Q. Wang, X.-X. Wang, X. Hu, M.-S. Xie, G.-R. Qu, H.-M. Guo, *Org. Lett.* **2014**, *16*, 2014–2017; f) M. Hennig, K. Püntener, M. Scalone, *Tetrahedron: Asymmetry* **2000**, *11*, 1849–1858; g) Z. Ding, J. Yang, T. Wang, Z. Shen, Y. Zhang, *Chem. Commun.* **2009**, 571–573; h) B. Zhang, M.-H. Xu, G.-Q. Lin, *Org. Lett.*, **2009**, *11*, 4712–4715; i) G. Kumaraswamy, D. Rambabu, *Tetrahedron: Asymmetry* **2013**, *24*, 196–201; j) K. Leijondahl, A.-B. L. Fransson, J.-E. Bäckvall, *J. Org. Chem.* **2006**, *71*, 8622–8625; k) N. J. Alcock, I. Mann, P. Peach, M. Wills, *Tetrahedron: Asymmetry* **2002**, *13*, 2485–2490; l) I. C. Lennon, J. A. Ramsden, *Org. Process Res. Dev.* **2005**, *9*, 110–112; m) T. Kioke, K. Murata, T. Ikariya, *Org. Lett.* **2000**, *2*, 3833–3836.
- [6] For relevant reviews see: a) J. Barrios-Rivera, Y. Xu, M. Wills, *Org. Biomol. Chem.* **2019**, *7*, 1301–1321; b) F. Foubelo, C. Nájera, M. Yu, *Tetrahedron: Asymmetry* **2015**, *26*, 769–790; c) A. Zoabi, S. Omar, R. Abu-Reziq, *Eur. J. Org. Chem.*, **2015**, 2101–2109; d) J. G. Deng, Y. Q. Tu, S. H. Wang, *Chem. Commun.* **2004**, 2070–2071; e) P. N. Liu, P. M. Gu, J. G. Deng, Y. Q. Tu, Y. P. Ma, *Eur. J. Org. Chem.* **2005**, 3221–3227; f) R. N. Liu, P. M. Gu, F. Wang, Y. Q. Tu, *Org. Lett.* **2004**, *6*, 169–172; g) R. Liu, T. Cheng, L. Kong, C. Chen, G. Liu, H. Li, *J. Catal.* **2013**, *307*, 55–61; h) J. Li, Y. Zhang, D. Han, Q. Gao, C. Li, *J. Mol. Catal. A* **2009**, *298*, 31–35; i) X. Huang, J. Y. Ying, *Chem. Commun.* **2007**, 1825–1827; j) D. Zhang, J. Xu, Q. Zhao, T. Cheng, G. Liu, *ChemCatChem* **2014**, *6*, 2998–3003.
- [7] a) R. Wang, J. Wan, X. a, X. Xu, L. Liu, *J. Chem. Soc. Dalton Trans.* **2013**, *42*, 6513–6522; b) X. Xu, R. Wang, J. Wan, X. Ma, J. Peng, *RSC Adv.* **2013**, *3*, 6747–6751; c) N. Haraguchi, K. Tsuru, Y. Arakawa, S. Itsuno, *Org. Biomol. Chem.* **2009**, *7*, 69–75; d) R. Marcos, C. Jimeno, M. A. Perciàs, *Adv. Synth. Catal.* **2011**, *353*, 1345–1352; e) R. Akiyama, S. Kobayashi, *Angew. Chem. Int. Ed.* **2002**, *41*, 2602–2604; *Angew. Chem.* **2002**, *114*, 2714–2716; f) Y. Arakawa, A. Chiba, N. Haraguchi, S. Itsuno, *Adv. Synth. Catal.* **2008**, *350*, 2295–2304; g) C. M. Zammit, M. Wills, *Tetrahedron: Asymmetry* **2013**, *24*, 844–852.
- [8] a) W. Shan, F. Meng, Y. Wu, F. Mao, X. Li, *J. Organomet. Chem.* **2011**, *696*, 1687–1690; b) J. Liu, Y. Zhou, Y. Wu, X. Li, A. S. C. Chan, *Tetrahedron: Asymmetry* **2008**, *19*, 832–837; c) H. F. Zhou, Q. H. Fan, Y. Y. Huang, L. Wu, Y. M. He, W. J. Tang, L. Q. Gu, A. S. C. Chan, *J. Mol. Catal. A* **2007**, *275*, 47–53; d) Y. Wu, C. Lu, W. Shan, X. Li, *Tetrahedron: Asymmetry* **2009**, *20*, 584–587.
- [9] a) X. Li, X. Wu, W. Chen, F. E. Hancock, F. King, J. Xiao, *Org. Lett.* **2004**, *6*, 3321–3324; b) X. Li, W. Hems, F. King, J. Xiao, *Tetrahedron Lett.* **2004**, *45*, 951–953.
- [10] J. M. Zimbron, M. Dauphinais, A. B. Charette, *Green Chem.* **2015**, *17*, 3255–3259.

- [11] a) I. Kawasaki, K. Tsunoda, T. Tsuji, T. Yamaguchi, H. Shibuta, N. Uchida, M. Yamashita, S. Ohta, *Chem. Commun.* **2005**, 2134–2135; b) T. J. Geldbach, P. J. Dyson, *J. Am. Chem. Soc.* **2004**, *126*, 8114–8115.
- [12] a) Y. C. Chen, T. F. Wu, L. Jiang, J. G. Deng, H. Liu, J. Zhu, Y. Z. Jiang, *J. Org. Chem.* **2005**, *70*, 1006–1010; b) W. Liu, X. Cui, L. Cun, J. Zhu, J. Deng, *Tetrahedron: Asymmetry* **2005**, *16*, 2525–2530.
- [13] a) Y. Zhao, R. Jin, Y. Chan, Y. Li, J. Lin, G. Liu, *RSC Adv.* **2017**, *7*, 22592–22598; b) G. Zhang, T. Liu, Y. Chou, Y. Wang, T. Cheng, G. Liu, *ChemCatChem* **2018**, *10*, 1882–1888; c) M. Gao, F. Chang, S. Wang, Z. Liu, Z. Zhao, G. Liu, *J. Catal.* **2019**, *370*, 191–197; d) J. Meng, F. Chang, Y. Su, R. Liu, T. Cheng, G. Liu, *ACS Catal.* **2019**, *9*, 8693–8701.
- [14] S. B. Wendicke, E. Burris, R. Scopelliti, K. Severin, *Organometallics* **2003**, *22*, 1894–1897.
- [15] T. Cheng, Q. Zhao, D. Zhang, G. Liu, *Green Chem.* **2015**, *17*, 2100–2122.
- [16] S. H. Yang, S. Chang, *Org. Lett.* **2001**, *3*, 2089–2091.
- [17] Y. Na, S. Chang, *Org. Lett.* **2000**, *2*, 1887–1889.
- [18] P. J. Dyson, D. J. Ellis, T. Welton, *J. Am. Chem. Soc.* **2002**, *124*, 9334–9335.
- [19] a) U. Karlsson, G.-Z. Wang, J.-E. Bäckvall, *J. Org. Chem.* **1994**, *59*, 1196–1198; b) M. Lee, S. Chang, *Tetrahedron Lett.* **2000**, *41*, 7507–7510.
- [20] a) D. L. Davies, J. Fawcett, S. A. Garratt, D. R. Russell, *Organometallics* **2001**, *20*, 3029–3034; b) J. W. Faller, B. J. Grimmond, *Organometallics* **2001**, *20*, 2454–2458; c) D. L. Davies, J. Fawcett, S. A. Garratt, D. A. Russell, *Chem. Commun.* **1997**, 1352–1352.
- [21] a) F. Simal, A. Demonceau, A. F. Noels, *Tetrahedron Lett.* **1998**, *39*, 3493–3496; b) F. Simal, D. Jan, A. Demonceau, A. F. Noels, *Tetrahedron Lett.* **1999**, *40*, 1653–1656.
- [22] S. Doherty, C. R. Newman, R. K. Rath, M. Nieuwenhuyzen, J. G. Knight, W. Clegg *Organometallics* **2005**, *24*, 2633–2644.
- [23] For ring closing metathesis see: a) E. L. Dias, R. H. Grubbs, *Organometallics* **1998**, *17*, 2758–2767; b) A. Fürstner, M. Picquet, C. Bruneau, P. H. Dixneuf, *Chem. Commun.* **1998**, 1315–1316; c) A. Fürstner, M. Liebl, C. W. Lehmann, M. Picquet, R. Kunz, C. Bruneau, D. Touchard, P. H. Dixneuf, *Chem. Eur. J.* **2000**, *6*, 1847–1857; d) A. Fürstner, L. Ackermann, *Chem. Commun.* **1999**, 95–96. For ring-opening metathesis see; e) A. Hafner, A. Mühlebach, P. A. van der Schaaf, *Angew. Chem. Int. Ed. Engl.* **1997**, *36*, 2121–2124; f) A. Demonceau, A. W. Stumpf, E. Saive, A. F. Noels, *Macromolecules* **1997**, *30*, 3127–3136; g) A. W. Stumpf, E. Saive, A. Demonceau, A. F. Noels, *J. Chem. Soc. Chem. Commun.* **1995**, 1127–1128.
- [24] a) T. Touge, T. Hakamata, H. Nara, T. Kobayashi, N. Sayo, T. Saito, Y. Kayaki, T. Ikariya, *J. Am. Chem. Soc.* **2011**, *133*, 14960–14963; b) P. Mörschel, J. Janikowski, G. Hilt, G. Frenking, *J. Am. Chem. Soc.* **2008**, *130*, 8952–8966.
- [25] T. Meng, Q.-P. Qin, Z.-L. Chen, H.-H. Zou, K. Wang, F.-P. Liang, *Dalton Trans.* **2019**, *48*, 5352–5360.
- [26] J. Soleimannejad, C. White, *Organometallics* **2005**, *24*, 2538–2541.
- [27] B. Therrien, G. Süß-Fink, *Inorg. Chim. Acta* **2006**, *359*, 4350–4354.
- [28] F. Martínez-Peña, S. Infante-Tadeo, A. Habtemariam, A. M. Pizarro, *Inorg. Chem.* **2018**, *57*, 5657–5668.
- [29] a) K.-J. Haack, S. Hashiguchi, A. Fujii, T. Ikariya, R. Noyori, *Angew. Chem. Int. Ed.* **1997**, *36*, 285–288; *Angew. Chem.* **1997**, *109*, 297–300; b) N. Uematsu, A. Fujii, S. Hashiguchi, T. Ikariya, R. Noyori, *J. Am. Chem. Soc.* **1996**, *118*, 4916–4917.
- [30] B. Vilhanová, J. Václavík, P. Šot, J. Pecháček, J. Zápál, R. Pažout, J. Maixner, M. Kuzma, P. Kačer, *Chem. Commun.* **2016**, *52*, 362–365.
- [31] J. Soleimannejad, A. Sisson, C. White, *Inorg. Chim. Acta* **2003**, *352*, 121–128.
- [32] a) S. Bai, H. Yang, P. Wang, J. Gao, B. Li, Q. Yang, C. Li, *Chem. Commun.* **2010**, *46*, 8145–8147; b) H. Yang, J. Li, J. Yang, Z. Liu, Q. Yang, C. Li, *Chem. Commun.* **2007**, 1086–1088.
- [33] a) J. M. Thomas, T. Maschmeyer, B. F. G. Johnson, D. S. Shepard, *J. Mol. Catal. A* **1999**, *141*, 139–144; b) F. Goettmanna, C. Sanchez, *J. Mater. Chem.* **2007**, *17*, 24–30; c) V. Mouarraris, R. Plessius, J. I. van der Vlugt, J. N. H. Reek, *Frontiers in Chem.* **2018**, *6*, 623.
- [34] B. Pugin, *J. Mol. Catal. A* **1996**, *107*, 273–279.
- [35] a) M. Yamakawa, I. Yamada, R. Noyori, *Angew. Chem. Int. Ed.* **2001**, *40*, 2818–2821; *Angew. Chem.* **2001**, *113*, 2900–2903; b) D. J. Morris, A. M. Hayes, M. Wills, *J. Org. Chem.* **2006**, *71*, 7035–7044.
- [36] A. M. R. Hall, P. Dong, A. Codina, J. P. Lowe, U. Hintermair, *ACS Catal.* **2019**, *9*, 2079–2090.
- [37] L. Vieille-Petit, B. Therrien, G. Süß-Fink, *Eur. J. Inorg. Chem.* **2003**, *20*, 3707–3711.
- [38] R. C. Clark, J. S. Reid, *Acta Crystallogr.* **1995**, *A51*, 887–897.
- [39] CrysAlisPro, Rigaku Oxford Diffraction, Tokyo, Japan.
- [40] G. M. Sheldrick, *Acta Crystallogr.* **2015**, *A71*, 3–8.
- [41] G. M. Sheldrick, *Acta Crystallogr.* **2008**, *A64*, 112–122.
- [42] O. V. Dolomanov, L. J. Bourhis, R. J. Gildea, J. A. K. Howard, H. Puschmann, *J. Appl. Crystallogr.* **2009**, *42*, 339–341.

Manuscript received: October 12, 2020
Revised manuscript received: November 20, 2020
Accepted manuscript online: December 2, 2020